

Frustrated Superexchange Interaction Versus Orbital Order in a LaVO_3 Crystal

J.-S. Zhou,¹ Y. Ren,² J.-Q. Yan,³ J. F. Mitchell,⁴ and J. B. Goodenough¹

¹*Texas Materials Institute, University of Texas at Austin, Austin, Texas 78712, USA*

²*Advanced Photon Source, Argonne National Laboratory, Argonne, Illinois 60439, USA*

³*Ames Laboratory, Ames, Iowa 50011, USA*

⁴*Material Science Division, Argonne National Laboratory, Argonne, Illinois 60439, USA*

(Received 14 December 2006; published 28 January 2008)

Measurements of magnetic, transport properties, thermal conductivity, and magnetization under pressure as well as neutron diffraction have been made on a single crystal and powder sample of LaVO_3 . The Néel temperature was found to mark a transition from the phase with both frustrated superexchange interaction and spin-orbit $\lambda\mathbf{L} \cdot \mathbf{S}$ coupling to the phase where the Jahn-Teller orbital-lattice coupling dominates. The dramatic reduction of absolute entropy in the paramagnetic phase is explained in terms of forming a long-range coherent state due to the interference between frustrated orbits and spins.

DOI: [10.1103/PhysRevLett.100.046401](https://doi.org/10.1103/PhysRevLett.100.046401)

PACS numbers: 71.70.Ej, 75.10.Dg, 75.30.Et, 75.50.Ee

In a magnetic insulator with orbital degeneracy, spin may couple to orbit through two terms: i.e., the interaction $\lambda\mathbf{L} \cdot \mathbf{S}$ in the case where the orbital angular momentum is not quenched and the quantum effect due to the frustrated superexchange interaction implied in the Kugel-Khomskii (KK) Hamiltonian [1]

$$H = \sum_{i,j'} H_{\text{orb}}^{i,j} \left(s_i \cdot s_j + \frac{1}{4} \right)$$

where $H_{\text{orb}}^{i,j}$ are operators in the orbital space. The $\lambda\mathbf{L} \cdot \mathbf{S}$ coupling provides an *intrasite* coupling as documented in transition-metal compounds [2]. The ground state of the KK Hamiltonian is realized by minimizing the energy in the joint spin and orbital space, which provides the *inter-site* magnetic coupling. Two perovskite families, RTiO_3 and RVO_3 , are good candidates possibly to show this nonclassic magnetic interaction. However, the community is split on whether in the RVO_3 perovskite family with two t_2 electrons, the dynamics of the spins and orbitals are determined by the superexchange interaction given a full orbital degree of freedom or by the orbital-lattice coupling. The essential assumptions and conclusions from a model [3,4] representing the first opinion include: (a) One t_2 electron is ordered into an xy orbital below a structural transition temperature T_{str} , which occurs below T_N in LaVO_3 and CeVO_3 but above T_N in the RVO_3 ($R = \text{Pr} \dots \text{Lu}$). (b) The other t_2 electron remains fluctuating between yz and zx orbitals to the lowest temperature for $R = \text{La} - \text{Tb}$, and to $T_{\text{str}}^* = T_{\text{CG}}$ for $R = \text{Dy} \dots \text{Lu}$, which provides the novel ferromagnetic interaction along the c axis. On the other hand, most experimentalists [5–8] and a few theorists [9,10] believed that the local structural distortion is large enough to lift the orbital degeneracy and to order one t_2 electron into the xy orbital at a temperature $T > T_{\text{OO}}$. The classic type- G orbital ordering for the second t_2 electron takes place at T_{OO} and undergoes an orbital

flipping transition at T_{CG} for the RVO_3 , $R = \text{Dy} \dots \text{Lu}$. However, LaVO_3 is exceptional in the RVO_3 family; the local structural distortion [11] in the paramagnetic phase is as small as that in LaFeO_3 and CaTiO_3 . It is widely accepted that the superexchange interaction, not the lattice-orbital interaction, dominates the dynamics of spins and orbitals in the paramagnetic phase. Moreover, although it is negligible in other RVO_3 , the spin-orbit coupling $\lambda\mathbf{L} \cdot \mathbf{S}$ also competes with a frustrated superexchange interaction in the paramagnetic phase of LaVO_3 . Two issues about this compound are still under hot debate: (a) whether orbital ordering takes place at T_N in addition to spin ordering and (b) whether the classic orbital ordering dominates the spin-spin interaction at $T < T_t$. Unfortunately, a thorough characterization of LaVO_3 is not available in the literature. In this Letter, we report high-resolution measurements of magnetic susceptibility, resistivity, thermoelectric power, thermal conductivity, magnetization under high pressure, and neutron diffraction on high-quality single-crystal and powder samples of LaVO_3 . The results not only are critical to distinguish between the existing models, but also to demonstrate new features due to a nonclassic magnetic interaction in the paramagnetic phase.

The single-crystal sample was grown with the floating-zone method. Pieces from the same ingot had been used for the structural study [6]. The atomic ratio La/V has been determined to be 0.99 ± 0.005 by ICP spectroscopy. This ratio and the mobile charge concentration 0.00016 as checked by the thermoelectric power measurement at room temperature confirm the nearly perfect oxygen stoichiometry of the crystal. The magnetization measurements were carried out in a commercial SQUID magnetometer (Quantum Design). All other measurements of transport properties were made on homemade apparatus. A miniature Be-Cu cell fitting into a commercial SQUID magnetometer was used to measure the dc magnetization. The compressibility of LaVO_3 was determined in a diamond

anvil cell mounted on a four-circle diffractometer (Bruker P4).

Miyasaka *et al.* [8] have reported magnetization, resistivity, lattice parameters, and specific heat on a single-crystal sample in a temperature range covering $T_N \approx 144$ K and $T_I \approx 141$ K. However, the LaVO_3 sample they used is about 9% hole doped as characterized chemically in the Letter. The resistivity is lower by 3 orders of magnitude than that of our crystal. With the definition shown in Fig. 1, we obtained $T_N = 145.5$ K and $T_I = 143.7$ K from the zero-field-cooled (ZFC) $\chi(T)$ of the crystal. T_N corresponds to the temperature where there is an upturn of $\kappa(T)$ from a glassy $\kappa(T)$ at $T > T_N$; T_I marks precisely the temperature where a big spike in $\kappa(T)$ occurs. $\rho(T)$ exhibits two discontinuous transitions in this temperature range. The interval between these two first-order transitions shown in the $\rho(T)$ data is the same as that from $T_N - T_I$ obtained from $\chi(T)$. Since a spin-ordering transition alone does not lead to a discontinuous change in $\rho(T)$, a first-order transition at T_N means a structural change as well as spin ordering. The upturn of $\kappa(T)$ at T_N is similar to the behavior of $\kappa(T)$ observed at the orbital ordering temperature T_{OO} in the $R\text{VO}_3$ ($R = \text{Pr} \dots \text{Lu}$) [12]. However, our results of transport and thermal conductivity properties cannot distinguish the following two possible pictures of what happens at T_N and T_I : (a) one t_2 electron is ordered into the xy orbital together with spin ordering at T_N followed by ordering of the second t_2

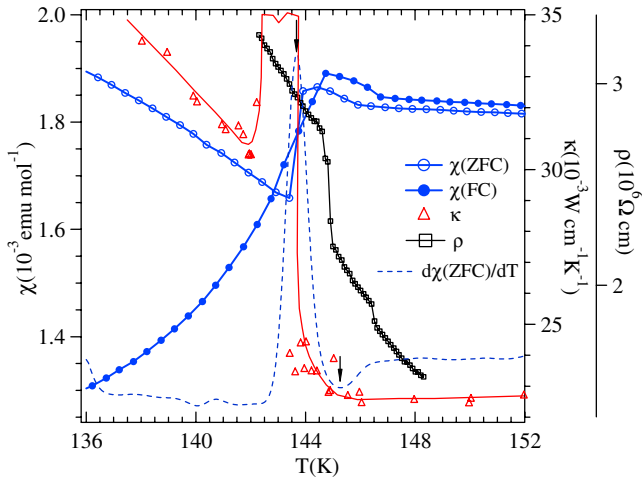


FIG. 1 (color online). The temperature dependences of the magnetic susceptibility $\chi(T)$ measured with $H = 1000$ Oe, thermal conductivity $\kappa(T)$ and resistivity $\rho(T)$ in the vicinity of T_N and T_I of the LaVO_3 crystal. T_N and T_I are defined, respectively, as a minimum and a peak in the $d\chi/dT$ curve shown by arrows inside the figure. We show the truncated spike of $\kappa(T)$ near T_I in order to have a smaller scale to show in detail how $\kappa(T)$ behaves near T_N . The line through the $\kappa(T)$ data is a guide to the eye. A slight shifting of transition temperatures T_N and T_I as monitored by the resistivity measurement relative to that from $\chi(T)$ may be caused by a small thermal gradient between the thermometer and the sample.

electron into yz or zx at T_I ; (b) type- C orbital ordering (C_{OO}) together with the corresponding type- G spin ordering (G_{SO}) are established at T_N , and they convert into the G_{OO}/C_{SO} phase at T_I . The specific type of orbital ordering in the possibility (b) is based on the C_{SO} from neutron diffraction [13] at temperatures well below T_I , which corresponds to G_{OO} according to the Goodenough-Kanamori rule. A distinct difference between these two possibilities is whether there is a spin flipping transition at T_I . A recent neutron diffraction result of Fig. 2 shows that the magnetic moment on V^{3+} obtained by fitting diffraction peaks with C_{SO} structure below T_I collapses abruptly at T_I . Although new magnetic diffractions appear within the interval between T_I and T_N that are too weak to resolve a possible spin structure, this observation indicates unambiguously that spins are ordered below T_N in a way different from that below T_I , which supports the second solution of spin and orbital ordering at T_N and T_I . We will further test the possible picture for the transitions at T_N and T_I by their pressure dependence.

As shown in Fig. 3, the ZFC $\chi(T)$ below T_I changes dramatically at low pressures. Moreover, the pressure dependences of T_N and T_I are nonlinear in this pressure range. We have made a linear fitting to the pressure dependences of T_N and T_I for $P > 2.2$ kbar where all the ZFC $\chi(T)$ show identical features. This high-pressure study reveals several important features about the transitions at T_N and T_I . (a) The dT_N/dP from the ZFC $M(T)$ is significantly higher than that predicted by the Bloch rule [14] $dT_N/dP = 3.3\kappa_c T_N$, where κ_c is the compressibility, which holds widely for antiferromagnetic insulators. (b) Both T_N and T_I obtained from the ZFC and FC $\chi(T)$

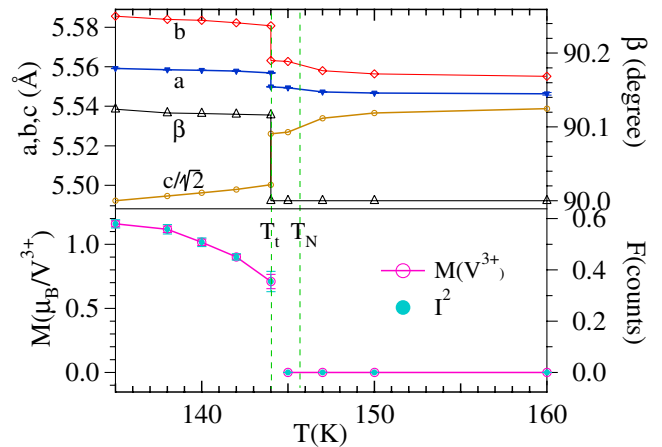


FIG. 2 (color online). Temperature dependences of lattice parameters and magnetic moment on V^{3+} ion obtained from the refinement (GSAS program) of the neutron powder diffraction of LaVO_3 . The C_{SO} structure was applied in refining the magnetic moment. F denotes the squared root of the integrated intensity of (100) and (010) magnetic reflections at $d \sim 5.5 \text{ \AA}$ for the C_{SO} structure. The neutron diffraction experiment was carried out at the Intense Pulsed Neutron Source, Argonne National Laboratory.

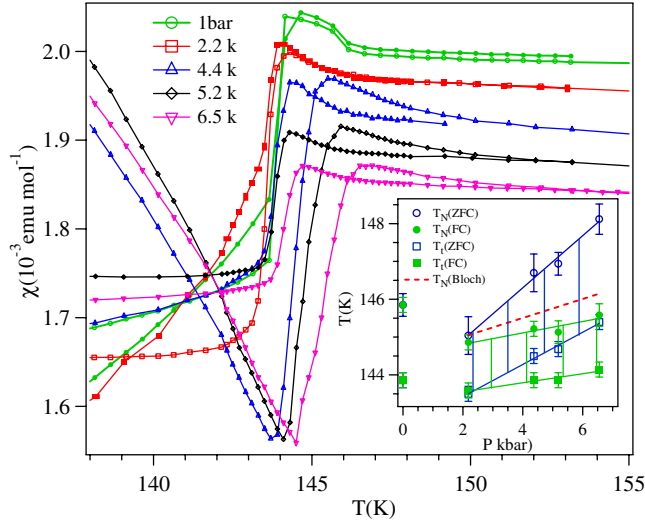


FIG. 3 (color online). The temperature dependence of magnetic susceptibility with $H = 5000$ Oe under different pressures. T_N and T_I are defined in the same way as shown in Fig. 1. The dashed line in the inset is from prediction by the Bloch rule based on the compressibility $k = 0.526 \times 10^{-3}$ kbar $^{-1}$ of LaVO $_3$ obtained in this work.

curves split under pressure. (c) Pressure enhances the interval $\Delta T = T_N - T_I$ for the ZFC $\chi(T)$ measurement, but makes no change for the FC measurement. The pressure-induced splitting at T_N between the FC and ZFC $\chi(T)$ has also been observed in CeVO $_3$ where a T_I is located below T_N . However, this effect disappears abruptly once the T_{OO} is higher than T_N [15]. These observations suggest that the splitting of T_N between the ZFC and FC measurements is characteristic of the magnetic transition in the phase with a frustrated superexchange interaction. The theoretical solution of the KK Hamiltonian with full orbital degree of freedom does not give a classic spin ordering at finite temperature [16]. A first-order transition at T_N as seen from $\rho(T)$ and corresponding change of $\kappa(T)$ would mean that degrees of freedom in both spin and orbital spaces are quenched or partially quenched. Although the volume changes at T_I and T_N as seen from the synchrotron study are still within error bars [6], the significant enhancement of T_N in the ZFC measurement reflects that pressure prefers the orbitally ordered phase below T_N relative to the orbitally disordered phase at $T > T_N$. A smaller pressure dependence of T_I than that of T_N is consistent with a small volume difference between two orbitally ordered phases on crossing T_I . The Bloch rule gives a change of T_N through a gain of the orbital overlap integral under pressure, whereas the transition at T_N in LaVO $_3$ is associated with quenching the orbital/spin degree of freedom. Therefore, the Bloch rule breaks down in this case.

The temperature dependence of thermal conductivity $\kappa(T)$ of LaVO $_3$ is shown in Fig. 4. Superimposed in the plot is the $\kappa(T)$ of the perovskite LaGaO $_3$ where there is no

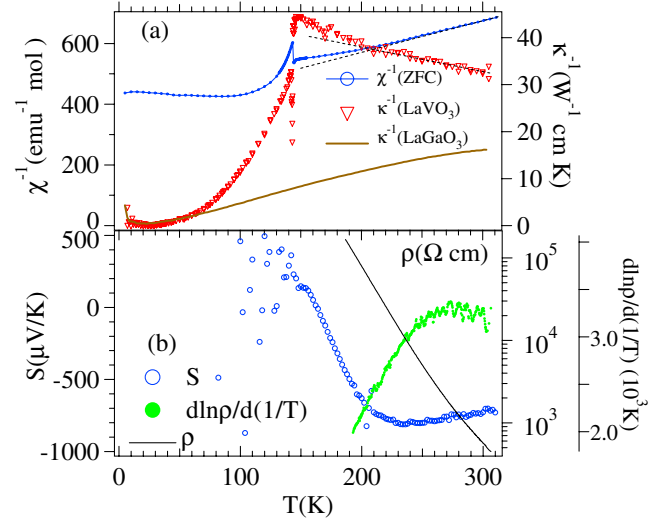


FIG. 4 (color online). Temperature dependence of the inverse dc magnetic susceptibility χ^{-1} , inverse thermal conductivity κ^{-1} , resistivity ρ and $d \ln \rho / d(1/T)$, and thermoelectric power S of single crystals LaVO $_3$ and LaGaO $_3$ [for $\kappa^{-1}(T)$ only].

spin, mobile charge, or Jahn-Teller active ion. LaGaO $_3$ exhibits not only qualitatively the typical phonon thermal conductivity, but also the upper bound of $\kappa(T)$ for perovskite oxides as far as we know. The low and glassy $\kappa(T)$ at $T > T_N$ is nicely consistent with a phase with a frustrated superexchange interaction. However, $\kappa(T)$ changes at T_N followed by a sharp increase at T_I in Fig. 1; it approaches the $\kappa(T)$ of LaGaO $_3$ as temperature decreases from T_I and overlaps with $\kappa(T)$ of LaGaO $_3$ at ~ 65 K. Therefore, there is no doubt that the phonon thermal conductivity is fully restored at $T < 65$ K. One may ask what is the relationship between the thermal conductivity and a magnetic interaction. Khaliullin [4] has made it clear that the orbital ordering state becomes “transparent” for the thermal phonons and y_z/z_x fluctuations enhance the phonon scattering. As mentioned in the introduction, the model by Khaliullin *et al.* gives a picture that the novel ferromagnetic interaction along the c axis is due to y_z/z_x fluctuations that supports the C_{SO} at $T < T_N$. A criteria for this model to work is a poor thermal conductivity lasting to the lowest temperature. The model has also predicted that the G_{SO} would result if the orbital became ordered at low temperature. What we have seen in Fig. 4, however, is a dramatic increase of $\kappa(T)$ below T_I , and there is no change of the magnetic susceptibility at $T = 65$ K. These observations are just opposite to that required by the frustrated superexchange model. In contrast, all our observations are consistent with the C_{OO}/G_{SO} phase below T_N and classic G_{OO}/C_{SO} phase below T_I , where the Jahn-Teller effect dominates. Nevertheless, the unusual transport properties in the paramagnetic phase do indicate that the frustrated superexchange interaction is in play above T_N .

A small and glassy $\kappa(T)$ in the paramagnetic phase is a solid proof that the orbitals are dynamically disordered. An unquenched orbital degree of freedom is essential to have

the frustrated superexchange interaction. It should also be noted that the glassy $\kappa(T)$ becomes even further reduced at $T < 220$ K. In order to find what makes the glassy $\kappa(T)$ even more suppressed, we turn to the measurements of transport properties in Fig. 4(b). A large and nearly temperature-independent thermoelectric power $S(T)$ at $T > 220$ K suggests that the statistical formula of Heikes for polaronic conduction is applicable to determine the mobile charge concentration. For the small polaron conduction, the statistical term, which is directly from the absolute entropy, dominates the thermoelectric power $S(T)$. On cooling through 220 K, the magnitude of $S(T)$ drops dramatically and approaches zero at $T \approx 160$ K, which indicates either an increase of mobile charge density from $c \approx 0.00016$ near room temperature to $c \approx 0.5$ at $T \approx 160$ K or that the mobile charges with a nearly constant density $c \approx 0.00016$ become strongly correlated over a large space. Since there is no charge reservoir in the perovskite structure and no structural transition occurs at 220 K [11], we can easily rule out the first possibility. The dramatic reduction of absolute entropy in the paramagnetic phase is significant; it signals the formation of a coherent state through the intersite spin-orbital coupling that excludes mobile electron from large-volume domains. It remains to be seen whether the model of a spin-orbital polaron [4] can account for this entropy reduction in the paramagnetic phase. The resistivity $\rho(T)$ in the entire temperature range of the paramagnetic phase cannot be fit by either a simple semiconducting formula $\rho(T) = \rho_0 \exp(E_g/k_B T)$ or the small polaron hopping formula $\rho(T) = T\rho_0 \exp(E_A/k_B T)$. The derivative $d \ln \rho(T)/d(1/T)$, which is normally related to the hopping energy E_A , shows a dramatic decrease at $T \approx 250$ K. Similar to the formation of Cooper pairs in a BCS superconductor, the long-range coherent state due to the intersite spin-orbital coupling carries less heat.

The inverse magnetic susceptibility $\chi^{-1}(T)$ curve of the paramagnetic phase also shows a slope change around 220 K. By fitting the $\chi(T)$ to the formula $\chi(T) = C/(T - \theta) + \chi_{\text{vV}} + \chi_{\text{dia}}$, which includes contributions from Curie-Weiss, Van Vleck χ_{vV} and the core diamagnetic χ_{dia} terms, we have obtained the unphysically large $\theta = 658$ K and 332 K in two temperature ranges $T_N < T < 220$ K and $220 \text{ K} < T < 310$ K, respectively. Since the exchange coupling between two V^{3+} ions on the diagonal direction of a cubic cell is negligible relative to that of a V-O-V bond, a $T_N \approx |\theta|$ is expected from classic antiferromagnetic theory. The observation of $|\theta| \gg T_N$ in the paramagnetic phase of the LaVO_3 crystal indicates that the CW law is invalid due to the presence of either spin-orbit $\lambda \mathbf{L} \cdot \mathbf{S}$ coupling as, for example, in the 9R polytype phase of BaRuO_3 [17] or the frustrated superexchange interaction. Therefore, the magnetic ordering at T_N in LaVO_3 is not a consequence of the magnetic coupling in the paramagnetic

phase, but rather through a structural transition that lowers the total energy in the joint spin and orbital spaces.

In conclusion, we have demonstrated five new results obtained on a high-quality LaVO_3 crystal that are directly related to the novel orbital physics in this compound: (a) Restoration of a phonon thermal conductivity qualitatively at $T < T_N$ and quantitatively at $T < 65$ K is fundamentally incompatible with the model in which the C_{SO} is caused by the yz/zx orbital fluctuations. (b) The C_{SO} collapses abruptly at T_i , which means that a different type spin ordering, most likely the G_{SO} , takes place at T_N . (c) The magnetic ordering in the phase with a frustrated superexchange interaction is characterized by a splitting between the ZFC and FC measurements that is strongly enhanced under pressure. (d) An unusually high pressure dependence of T_N and a discontinuous change of $\rho(T)$ at T_N also support that orbital ordering takes place at T_N . (e) The Curie-Weiss law fails to describe the temperature dependence of magnetic susceptibility in the paramagnetic phase of LaVO_3 . This failure can be caused either by a frustrated superexchange interaction or by spin-orbit $\lambda \mathbf{L} \cdot \mathbf{S}$ coupling. (f) The most surprising change in the paramagnetic phase is the dramatic reduction of absolute entropy starting near 220 K. It remains to be verified whether this change is due to developing a long-range coherent state as a solution of the KK Hamiltonian.

We thank the Robert A. Welch Foundation and the NSF for financial support. J.-S. Zhou thanks the hospitality by the Institute for Solid State Physics, University of Tokyo, where he refined the presentation of the manuscript. Work at Argonne National Laboratory was supported by the U.S. Department of Energy under Contract No. DE-AC02-06CH11357.

-
- [1] Z. Nussinov *et al.*, *Europhys. Lett.* **67**, 990 (2004).
 - [2] J. B. Goodenough, *Phys. Rev.* **171**, 466 (1968).
 - [3] G. Khaliullin *et al.*, *Phys. Rev. Lett.* **86**, 3879 (2001).
 - [4] G. Khaliullin, *Prog. Theor. Phys. Suppl.* **160**, 155 (2005).
 - [5] G. R. Blake *et al.*, *Phys. Rev. Lett.* **87**, 245501 (2001).
 - [6] Y. Ren *et al.*, *Phys. Rev. B* **67**, 014107 (2003).
 - [7] S. Miyasaka *et al.*, *Phys. Rev. B* **68**, 100406 (2003).
 - [8] S. Miyasaka *et al.*, *Phys. Rev. Lett.* **85**, 5388 (2000).
 - [9] Y. Motome *et al.*, *Phys. Rev. Lett.* **90**, 146602 (2003).
 - [10] M. De Raychaudhury *et al.*, *Phys. Rev. Lett.* **99**, 126402 (2007).
 - [11] P. Bordet *et al.*, *J. Solid State Chem.* **106**, 253 (1993).
 - [12] J.-Q. Yan *et al.*, *Phys. Rev. Lett.* **93**, 235901 (2004).
 - [13] V. G. Zubkov *et al.*, *Sov. Phys. Solid State* **18**, 1165 (1976) [*Liz. Tverd. Tela (Leningrad)* **18**, 2002 (1976)].
 - [14] D. Bloch, *J. Phys. Chem. Solids* **27**, 881 (1966).
 - [15] J.-S. Zhou *et al.*, *Phys. Rev. Lett.* **99**, 156401 (2007).
 - [16] A. B. Harris *et al.*, *Phys. Rev. Lett.* **91**, 087206 (2003).
 - [17] M. Drillon *et al.*, *J. Chem. Soc., Faraday Trans. 2* **75**, 1193 (1979).